Compatible ground-motion time histories for new national seismic hazard maps

Gail M. Atkinson and Igor A. Beresnev

Abstract: Ground-motion time histories which are compatible with the uniform hazard spectra (UHS) provided by the new national seismic hazard maps of the Geological Survey of Canada (GSC) are simulated. Time histories are simulated for the following cities: Halifax, La Malbaie, Québec, Montreal, Ottawa, Toronto, Prince George, Tofino, Vancouver, and Victoria. The target UHS for the time history simulations are the GSC 5% damped horizontal-component spectra for "firm ground" (Class B) sites for an annual probability of 1/500. The Canadian Council on Earthquake Engineering is currently considering the adoption of these maps as the seismological basis for the earthquake design requirements for future editions of the National Building Code of Canada. It is therefore useful to have compatible time histories for these spectra, in order that dynamic analysis methods requiring the use of time histories can be employed. The simulated records provide a realistic representation of ground motion for the earthquake magnitudes and distances that contribute most strongly to hazard at the selected cities and probability level. For each selected city, two horizontal components are generated for a moderate earthquake nearby, and two horizontal components are generated for a larger earthquake farther away. These records match the short- and long-period ends of the target UHS, respectively. These simulations for local and regional crustal earthquakes are based on a point-source stochastic simulation procedure. For cities in British Columbia, records are also simulated for a scenario **M**8.5 earthquake on the Cascadia subduction zone, using a stochastic finite-fault simulation model. Four different rupture scenarios are considered. The ground motions for this scenario event are not associated with a specific probability level, but current information suggests that their probability of occurrence is comparable to that of the 1/500 UHS (the probabilistic analyses performed for the national hazard maps do not explicitly include the Cascadia subduction event). Thus it would be reasonable to conduct engineering analyses for cities in British Columbia using both the simulated crustal-event motions and the simulated Cascadia-event motions for the Cascadia event. The time histories simulated for this study are available free of charge to all interested parties.

Key words: compatible time-histories, seismic hazard, ground motions.

Résumé : Des historiques des mouvements du sol qui sont compatibles avec un spectre uniforme de risques sismiques (SURS), fournis par les nouvelles cartes nationales de la séismicité de la Commission géologique du Canada (CGC) sont simulés. Ces historiques sont simulés pour les villes suivantes : Halifax, La Malbaie, Québec, Montréal, Ottawa, Toronto, Prince George, Tofino, Vancouver et Victoria. L'objectif du SURS pour les simulations temporelles est d'amortir le composant horizontal du spectre du CGC de 5% pour des sites de « sols compacts » (classe B) pour une probabilité annuelle de 1/500. Le conseil canadien d'ingénierie parasismique considère actuellement l'adoption de ces cartes comme une base sismologique pour les exigences en conception parasismique pour les futures éditions du Code national du bâtiment du Canada. Il s'avère donc utile de posséder des historiques compatibles pour ces spectres, afin que les méthodes d'analyse dynamique nécessitant l'utilisation d'historiques puissent être employées. Les cas simulés offrent une représentation réaliste des mouvements du sol pour des magnitudes et distances de tremblement de terres qui contribuent le plus fortement au risque des villes choisies et au niveau de probabilité. Pour chacune des villes précitées, deux composantes horizontales sont générées pour un tremblement de terre modéré à proximité, et deux autres composantes horizontales sont générées pour un tremblement de terre plus important mais également plus éloigné. Ces enregistrements concordent avec les termes sur une courte et sur une longue période du SURS visé respectivement. Ces simulations de séismes lithoshériques locaux et régionaux sont basées sur une procédure de simulation stochastique à source ponctuelle. En ce qui concernent les villes de la Colombie Britannique, les enregistrements sont aussi simulés pour un scénario d'un séisme **M**8,5 sur la zone de subduction de Cascadia, au moyen d'un modèle de simulation stochastique à défaut fini. Quatre différents scénarios de rupture furent considérés. Les mouvements du sol pour ces scénarios ne sont pas associés à un niveau de probabilité spécifique, mais les informations actuelles suggèrent que leur probabilité d'occurrence soit comparable au SURS 1/500 (l'analyse probabilistique réalisée pour les cartes de la séismicité du Canada n'inclut pas explicitement l'événement de subduction de Cascadia). Il serait donc raisonnable de mener des analyses techniques pour les villes de la Colombie Britannique, en utilisant à la fois les mouvements simulés

Received October 1, 1996. Revised manuscript accepted August 25, 1997.

G.M. Atkinson and I.A. Beresnev. Department of Earth Sciences, Carleton University, 1125 Colonel By Drive, Ottawa, ON K1S 5B6, Canada.

Written discussion of this article is welcomed and will be received by the Editor until August 31, 1998 (address inside front cover).

d'événements lithosphériques et ceux de la zone de subduction de Cascadia pour simuler l'événement de Cascadia. Les historiques simulés pour cette étude sont disponibles gratuitement à toute personne intéressée.

Mots clés : historiques compatibles, risque sismique, mouvement du sol.
[Traduit par la rédaction]

Introduction

New national seismic hazard maps have been developed by the Geological Survey of Canada (GSC) (Adams et al. 1996). The maps present 5% damped uniform-hazard response spectra (UHS) for firm ground sites for a number of vibrational periods, at a probability level of 1/500 per annum (p.a.). The Canadian Council on Earthquake Engineering (CANCEE) is currently considering the adoption of these new maps as the seismological basis for the earthquake design requirements for future editions of the National Building Code of Canada (NBCC). The new maps embody the last 15 years of progress in seismological information and seismic hazard analysis techniques, and are intended to replace the current zoning maps in the NBCC, which were developed around 1980.

For buildings to be designed either using the equivalent-lateral-force procedures of the NBCC or by a dynamic analysis using modal analysis procedures, the new hazard maps, used in conjunction with the NBCC provisions, provide all the required input information for the engineering analyses. In some cases, however, the engineer may wish to perform a dynamic analysis based on a time-history method. Time histories that are equivalent to the UHS given by the seismic hazard maps are required for such applications; these ground motion records are referred to as compatible time histories.

Obtaining UHS-compatible time histories is not a trivial task, particularly for the Canadian seismic hazard environment. One approach is to select real recordings that match the "target" spectrum in a selected period range. However, this approach is only appropriate when recordings are available for the magnitude–distance range and tectonic environment that is causing the hazard. If these conditions cannot be met, then the selected real records will have no clear relationship to the ground motion hazard at the site; the motions may not be physically realizable in terms of frequency content or duration of motion, for example. Unfortunately, this is the situation for most of Canada. In particular, for the magnitude–distance combinations identified in this study as representative of the GSC 1/500 spectra (Table 1), there are no applicable records for either eastern or western Canada. Use of California records to represent these events would be inappropriate; there are pervasive differences in source, attenuation, and site characteristics between California earthquakes and those in eastern and western Canada, which profoundly affect the amplitudes and frequency content of the ground motions (Atkinson 1995*a*, 1995*b*; Atkinson and Boore 1997*b*). Thus "real" earthquake recordings from California cannot provide "real" records for Canada.

The alternative in this situation is to simulate suitable records. It is important that the simulation technique be capable of generating physically realizable records. There are some well-used engineering simulation programs that generate a compatible time history directly from a specified response spectrum (based on no other seismological information). If these approaches are applied to a uniform-hazard spectrum, they produce an artificial composite record which is unlike any actual ground motion that might be experienced; the composite record is more akin to the simultaneous occurrence of a number of potentially damaging events. To produce physically realistic time histories, it is necessary to simulate motions which not only match the spectrum, but which are representative of motions for specific magnitude–distance scenarios in the region of interest. Such simulation procedures are well developed and frequently applied in design of critical facilities (e.g., Reiter 1990), but are not often employed for the analysis of ordinary structures.

There is, perhaps, an intuitive reluctance to substitute simulated time histories for real earthquake recordings. There are apparent differences between simulated and real records, reflecting factors such as non-stationarity of signals due to arrivals of different wave groups, unmodeled signal complexity, and unmodeled ground motion coda. These factors combine to make simulated records differ, visually, from many real recordings. Numerous studies have shown, however, that simulated records and real records are functionally equivalent, from both the linear and nonlinear points of view. For example, Greig and Atkinson (1993) compared elastic and inelastic strength demand spectra for 66 records from four eastern Canadian earthquakes (including the Saguenay, Quebec, earthquake of 1988), with the corresponding spectra for simulated records of the same events and distances. The real records varied in composition, from near-source records containing only direct waves, to distant records dominated by complex surface wave trains; the simulated records were stationary signals. These comparisons showed that the simulated records provided an adequate basis for estimating both linear and nonlinear effects. This is not surprising, because the real and simulated signals have approximately the same amplitude and frequency content, and approximately the same duration. Turkstra and Tallin (1988) reached a similar conclusion based on comparisons of simulated records with actual time histories for a number of California earthquakes.

On a philosophical note, it is important to recognize that recorded time histories are only "real time histories" in the sense that they represent a past event that actually happened. They will never be recorded again. Future events, having magnitudes, locations, and rupture characteristics different from those of past events, will produce records with different ground motion characteristics. The advantage of the simulation approach lies in generalizing the gross features of past events that are repeatable (e.g., average amplitudes and frequency content as a function of magnitude and distance), while building in an appropriate stochastic element to account for the features of ground motion which are random. In the context of their future likelihood of occurrence, simulated records are just as "real" as past recordings.

It is the purpose of this paper to simulate compatible time histories for the new 1/500 national seismic hazard maps, for

a number of cities in eastern and western Canada. The eastern hazard is derived from local moderate earthquakes and larger regional events, all within the shallow ($h < 30$ km) crust. For the western cities, time histories are simulated for crustal earthquakes, as well as for a **M**8.5 scenario earthquake along the Cascadia subduction zone.

Definition of scenario events for the simulations

Basis for scenario events

The starting point for the simulation of spectrum-compatible time histories is the definition of scenario events, in terms of earthquake magnitude and distance. These events should represent the types of earthquakes that are the dominant contributors to the seismic hazard at the site of interest, for the specified probability level. This study adopts the 1/500 p.a. uniform hazard spectra of Adams et al. (1996) as the foundation for this selection, for all crustal earthquakes.

Overview of GSC spectra

The spectra of Adams et al., hereafter referred to as the GSC spectra, were derived from a probabilistic hazard analysis, following the well-known Cornell–McGuire method (Cornell 1968; McGuire 1977; Toro and McGuire 1987; see EERI (1989) for a review). The basic steps of the analysis are as follows. First, seismotectonic information is used to define seismic source zones, which may be areas of diffuse or concentrated seismicity, or specific active faults. Generally, a number of alternative hypotheses regarding the configuration of these seismogenic source zones are formulated. For each source zone, the earthquake catalogue is used to define the magnitude–recurrence relation and its uncertainty; this provides the description of the frequency of occurrence of events within the zone, as a function of earthquake magnitude. Ground-motion relations are defined (along with their uncertainty) to provide the link between the occurrence of earthquakes within the zones, and the resulting ground motions at a specified location. Ground-motion relations can be given in terms of peak ground acceleration or velocity, or for response spectral ordinates for given periods of vibration. Within the last 10 years, practice has shifted to the use of response spectra instead of peak ground-motion parameters, due to their greater engineering relevance (EPRI 1986; EERI 1989; Atkinson 1991; Heidebrecht et al. 1994). Thus the GSC maps are based on response spectral ordinates.

The final step of the hazard analysis is an integration, over all earthquake magnitudes and distances, of the contributions to the probability of exceeding specified ground-motion levels at the site of interest. This is repeated for a number of vibrational periods in order to define the uniform-hazard spectrum, which is a response spectrum having a specified probability of exceedence. If an analysis of uncertainty has been carried throughout the analysis (as for the GSC spectra), then a family of spectra for each probability level can be defined, representing the confidence with which the probabilistic motions can be determined. These confidence limits are derived from the uncertainty in the model parameters that describe the hazard. Thus they represent model uncertainty, as opposed to random variability in the underlying physical processes. Note that random variability is considered explicitly in the hazard integrations, and its effects are thus included in the hazard curves for all confidence levels.

For critical facilities, one may wish to be 80% or 90% confident that the true hazard curve lies below the adopted value, and might therefore wish to use 80th or 90th percentile hazard curves. In the case of the GSC maps, the adopted spectra represent median values (e.g., 50th percentile) for ground motion with a probability of 1/500 p.a. Generally speaking, median hazard curves are similar to the "best-estimate" values that would be obtained if model uncertainty were not included in the analysis. The GSC spectra are defined for "firm ground" site conditions, representing Class B sites in the terminology of Boore et al. (1993); the average shear-wave velocity for such sites is given as 555 m/s.

Selecting compatible time histories

The uniform-hazard spectrum (UHS) can be thought of as a composite of the types of earthquakes that contribute most strongly to the hazard at the specified probability level. In general, the dominant contributor to the short-period ground-motion hazard comes from small-to-moderate earthquakes at close distances, whereas larger earthquakes at greater distance contribute most strongly to the long-period ground-motion hazard (Reiter 1990; McGuire 1995). As the probability level is lowered, the dominant effect is to move both the regional and local contributing earthquakes closer to the site.

To be compatible with the UHS, time histories should be simulated for the earthquake magnitudes and distances which dominate the seismic hazard for the selected probability level. Furthermore, the spectra for the selected records, when taken as a suite, should approximately match the target UHS response spectrum. These considerations suggest that more than one type of earthquake will generally be required to match the target spectrum over the entire period range of interest (assumed to be approximately 0.1–5 s). A typical example might be a target spectrum which is matched in the 0.1–0.5 s band by a moment magnitude (**M**) 5.5 earthquake at distance (R) of 20 km, and matched in the 0.5–5 s band by a **M**7 earthquake at $R = 70$ km. The moderate nearby earthquake would not produce sufficient long-period energy to match the 0.5–5 s band of the UHS, while the larger distant earthquake would have lost too much high-frequency energy, due to attenuation, to match the short-period band. Therefore the structure would need to be analyzed for both of these earthquakes, unless its range of response limits this requirement. Note that the peak ground acceleration of the motion is often not particularly relevant, as it is carried by the highest frequencies in the record, which may be above the frequency range of structural response. For example, magnitude 3 earthquakes can produce very large accelerations near the earthquake source, but these do not cause damage to structures.

A rigorous selection of representative earthquake magnitudes and distances can be made on a site-specific basis by "de-aggregating" the seismic hazard results (McGuire 1995). This procedure involves taking apart the integral in the probability calculations that sums the hazard contributions over magnitude, distance, and random variability in ground-motion amplitudes (sigma). The relative probability contributions are examined as functions of these parameters, for each vibrational period of interest. Time histories can then be selected or simu-

lated for the most-likely combinations of magnitude, distance, and sigma, for a certain period range.

Based on practical experience with these de-aggregations in a variety of tectonic environments (e.g., Atkinson 1990; McGuire 1995), the following simplified representation of this process is adopted:

- The 1/500 UHS for the modeled eastern Canadian sites can be adequately approximated using an event of **M**5.5 to represent the short-period hazard plus an event of **M**7.0 to represent the long-period hazard; the distances at which these events are placed depend on the seismicity rates of the site area.
- The 1/500 UHS for the modeled western Canadian cities (all in western B.C.) can be adequately approximated using an event of **M**6.0 to represent the short-period hazard plus an event of **M**7.2 to represent the long-period hazard; the distances at which these events are placed depend on the seismicity rates of the site area. These two scenario events represent only the hazard due to crustal and subcrustal earthquakes, and do not include the hazard due to a great earthquake along the Cascadia subduction zone.
- For the scenario crustal earthquakes in both eastern and western Canada, ground motions should be simulated for approximately the median-plus-one-standard-deviation ground-motion level (e.g., the median level times a factor of 2), for the stated magnitude and distance. The multiplicative factor of 2.0 on the amplitudes for the given magnitude and distance can be adjusted up or down somewhat (within about the range from 1.0 to 3.0) as needed to match the target spectrum. Note that the time histories so obtained are still representative of the *median* UHS, because this factor is applied before the time histories are matched to the target median UHS. (In other words, the spectra of the simulated events still match the median UHS.) The purpose of including the factor is to account for typical de-aggregation results, which show that the dominant hazard contributions come from motions that are larger-than-median for the given magnitude and distance (e.g., see McGuire 1995). This reflects amplitude variability in recorded ground motions, which is the most important factor influencing the relationship between median and 84th percentile motions.
- A great earthquake on the Cascadia subduction zone is treated as a separate scenario for western cities. This is consistent with the approach of the GSC; they did not include the Cascadia subduction event in the probabilistic computations of the UHS, but examined it as a separate "scenario" event. The adopted magnitude for this scenario is **M**8.5 in this paper, slightly larger than the value of **M**8.2 used by the GSC. Its probability of occurrence has not been explicitly evaluated, but is believed to be roughly comparable to the probability of the shallow crustal scenarios.

Simulated time histories for crustal earthquakes

Simulation methodology

The stochastic point-source simulation method of Boore (1983) is used to generate time histories for the crustal earthquakes in both eastern and western Canada. Both the method and its application to eastern and western Canada have been described in detail elsewhere (Atkinson and Boore 1995, 1997*a*) and will only be summarized here. The method has its origins in the observation that, on average, high-frequency ground motions can be accurately modeled as finite-duration bandlimited Gaussian noise, with an underlying Fourier amplitude spectrum as specified by a simple seismological model of source and propagation processes (Hanks and McGuire 1981; Boore 1983; Atkinson and Boore 1995).

Fig. 1. Amplification factor applied in the frequency-domain to convert simulations for hard-rock sites to simulations for Class B (firm ground) soil sites. These factors were applied to all simulations presented in this paper.

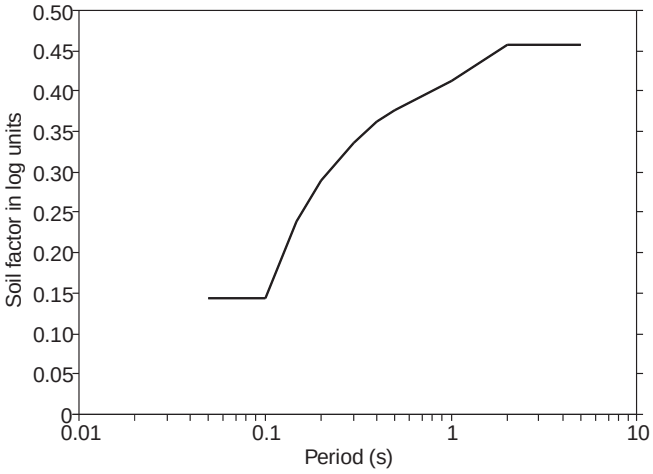

The method begins with the generation of a windowed acceleration time series, comprised of random Gaussian noise with zero mean amplitude, and a mean spectral amplitude of unity. The duration of the window is specified as a function of magnitude and distance, based on regional empirical observations. The spectrum of the windowed noise time series is multiplied by a desired Fourier acceleration spectrum; this spectrum is specified as a function of seismic moment (or moment magnitude, **M**) and distance, based on a seismological or empirical model. A point-source representation of source and propagation is used for the simulations of crustal events: this is readily justified for the magnitude–distance range of events that dominate the hazard at the 1/500 p.a. probability level. The filtered spectrum is then transformed back into the time domain to yield a simulated earthquake record for that magnitude and distance.

The Fourier amplitude spectrum used to control the amplitude and frequency content of the time history is a product of the source spectrum as a function of magnitude, its attenuation with distance, and the amplification by the local site conditions, as well as by the factor of 2 used to generate motions near the median-plus-one-standard-deviation level for the given **M** and R.

For this study, the object is to generate motions for "firm soil' conditions (Class B of Boore et al. 1993). The seismological models of source and propagation, which are used to generate the amplitude spectra, are applicable to hard rock conditions (shear-wave velocity of 2.5–3.5 km/s). This is because the seismograph stations, which recorded the empirical data on which these models were based, are sited almost exclusively on hard rock, in both eastern and western Canada.

Table 1. Applicable time histories to match GSC 1/500 p.a. target UHS.

City	Short-period event	Scale factor for short-period event	Long-period event	Scale factor for long-period event
Halifax; Toronto	**M**5.5 at R70	1.2	**M**7 at R300	0.6
La Malbaie	**M**5.5 at R15	1.3	**M**7 at R30	0.7
Québec; Montreal; Ottawa	**M**5.5 at R30	0.8	**M**7 at R150	0.7
Prince George	**M**6 at R70	0.7	**M**7.2 at R200	0.7
Vancouver; Victoria	**M**6 at R20	1.1	**M**7.2 at R70	0.8
Tofino	**M**6 at R30	1.0	**M**7.2 at R70	0.7

Fig. 2. Target 1/500 p.a. UHS from GSC for Halifax (filled squares) and Toronto (open squares), and spectra of selected compatible time histories, multiplied by the stated scaling factor (the geometric average of the spectra for two horizontal components for the stated **M** and *R* combination is plotted). Solid line shows spectra for event that matches the short-period end of the spectrum; dotted line shows spectra for event that matches the long-period end of the spectrum.

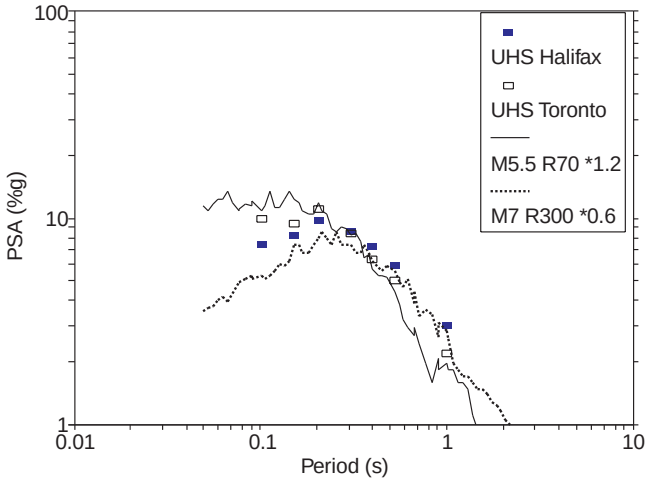

Fig. 3. Target 1/500 p.a. UHS from GSC for Québec (filled squares), Montreal (open squares), and Ottawa (asterisks), and spectra of selected compatible time histories, multiplied by the stated scaling factor (the geometric average of the spectra for two horizontal components for the stated **M** and *R* combination is plotted). Solid line shows spectra for event that matches the short-period end of the spectrum; dotted line shows spectra for event that matches the long-period end of the spectrum.

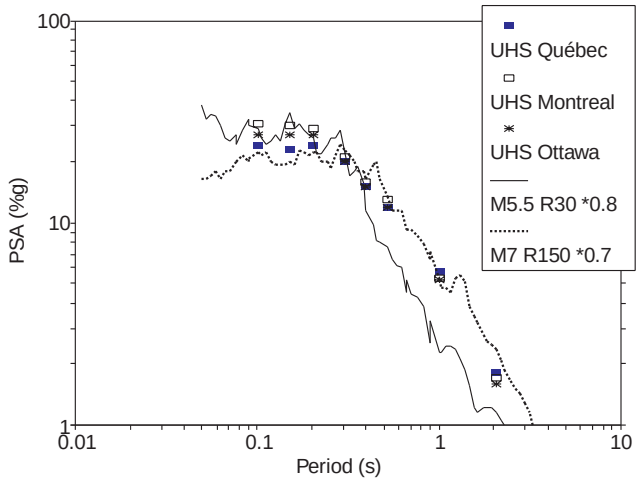

The amplitude spectra are therefore multiplied by the soil-amplification factors appropriate for Class B sites, shown in Fig. 1. These factors are adopted from Adams et al. (1996), and represent a synthesis of empirical and analytical soil response studies. The use of frequency-dependent amplification factors is consistent with the foundation-factor approach that is embodied in the NBCC and model U.S. codes (Martin and Dobry 1994; NEHRP 1994); it is also consistent with observations from California, where the ground-motion database is large enough to allow such factors to be derived empirically (e.g., Boore et al. 1993).

The soil amplification factors were derived to convert generic "hard-rock" motions to equivalent motions on Class B soils. In the methodology of Adams et al. they were only required for the eastern applications. In this study, they are also applied to the B.C. simulations, since the B.C. simulation methodology is based on hard-rock motions. The soil factors have been extended to periods (T) slightly beyond that given by Adams et al. by assuming constant amplification for $T < 0.1$ s and for $T > 2$ s. This is a conservative assumption, since amplifications eventually tend to unity at both the short- and long-period ends of the spectrum.

Eastern Canada

The stochastic point-source simulations for eastern Canada use the seismological model parameters of Atkinson and Boore (1995), as amplified by the soil factors shown in Fig. 1, and by the factor of 2 to generate median-plus-sigma amplitude levels for the specified **M** and *R*. The model was developed specifically for eastern North America, and the model parameters validated empirically using recordings from over 100 eastern earthquakes in the magnitude range from 3 to 6.8. In order to generate time histories that are compatible with the target UHS, magnitude–distance combinations are sought that will result in a match in median levels over the period band of interest — generally by using more than one record for the analysis, with different records covering different parts of the period band. Because the exact locations of peaks and troughs in the generated records are random, structures should be analyzed for more than one record. Accordingly, two time histories have been generated for each event; these can be considered as two random horizontal components of acceleration.

Time histories are generated for **M**5.5 and **M**7.0 earthquakes at hypocentral distances (R) of 15, 20, 30, 50, 70, 100,

Fig. 4. Target 1/500 p.a. UHS from GSC for La Malbaie (filled squares), and spectra of selected compatible time histories, multiplied by the stated scaling factor (the geometric average of the spectra for two horizontal components for the stated **M** and *R* combination is plotted). Solid line shows spectra for event that matches the short-period end of the spectrum; dotted line shows spectra for event that matches the long-period end of the spectrum.

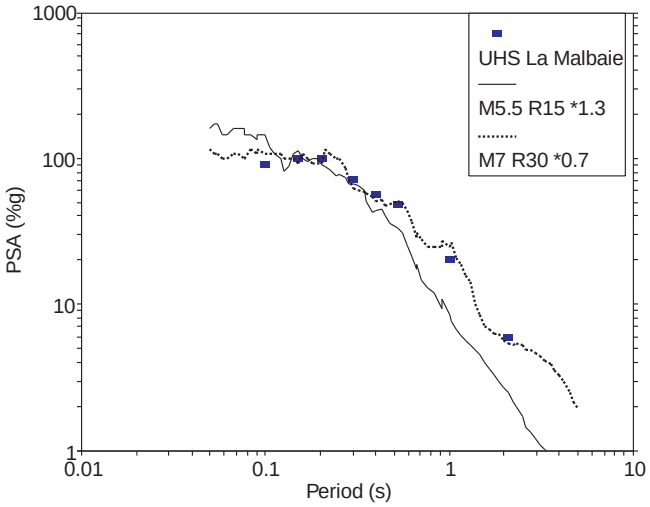

150, 200, and 300 km (for Class B sites, for motions a factor of two times the median levels). For each city, the best distance value for the **M**5.5 event is selected, such that the average spectrum for the two simulated records most closely matches the short-period end of the target UHS spectrum. Similarly, the best distance value for the **M**7.0 simulations is determined by matching the long-period end of the target UHS. The selected time histories are then scaled up or down by a "fine-tuning" factor (between 0.6 and 1.3), so as to match the target as closely as possible. This fine-tuning factor is equivalent to adjusting the number of standard deviations of the motion from the median, within the range from 1.2 to 2.6 standard deviations (e.g., 0.6×2 to 1.3×2). The selected events and fine-tuning factors are given in Table 1. Figures 2–4 show the target UHS spectra for the selected eastern cities, and the corresponding spectra for the simulated time histories, as scaled by the fine-tuning factor; the geometric average of the spectra of the two horizontal components is plotted.

There is significant overlap in the intermediate-period range between the spectra of the **M**5.5 and **M**7.0 events, but they may have different effects on the structure due to differences in overall duration and frequency content. In some cases the target spectra were considered simultaneously for two or more cities, due to the similarity of their UHS (e.g., target spectra are not significantly different for Ottawa, Montreal, and Québec). Figure 5 plots example time histories for the **M**5.5 and **M**7.0 events at selected distances. Notice that the **M**5.5 event has a shorter duration and higher frequency content than the more distant **M**7.0 event.

Western Canada (B.C.)

Simulations for the crustal or subcrustal events of **M**6.0 and **M**7.2 for B.C. are based on the same stochastic point-source simulation methodology used for eastern Canada. In this case, however, the seismological model of the earthquake Fourier

Fig. 5. Example time histories (unscaled) for eastern cities: (*a*) **M**5.5 event at $R = 20$ km and (*b*) **M**7 event at $R = 70$ km.

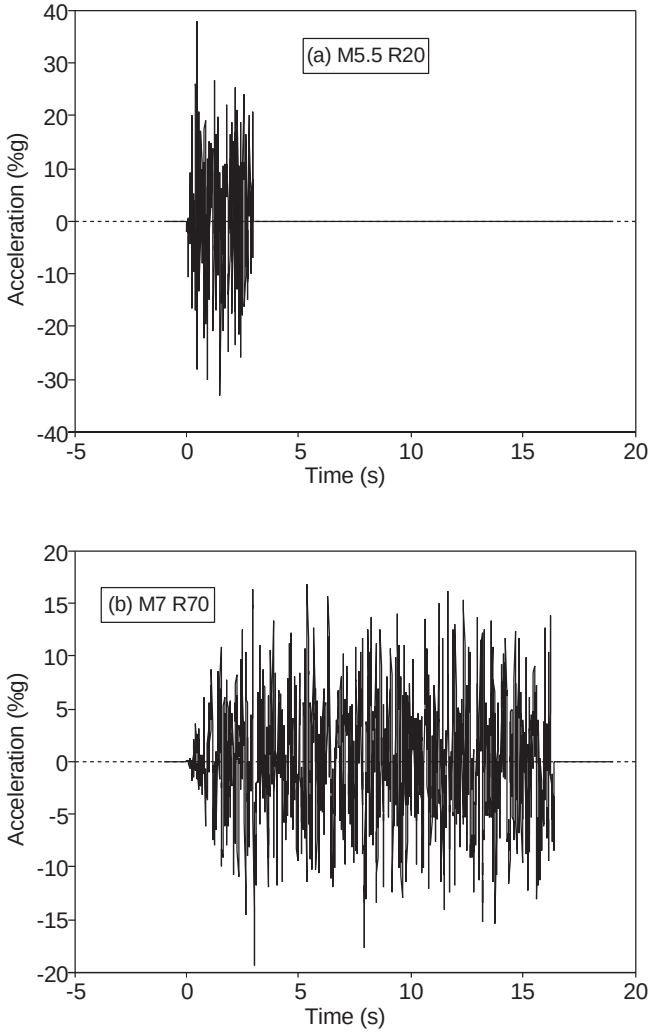

amplitude spectrum, as a function of magnitude and distance, and the duration model are specific to B.C. (Atkinson 1995*a*). These models were developed and empirically validated using records from about 60 B.C. earthquakes of magnitude 3.5 to 7 (see also Atkinson and Boore 1997*a*). High-frequency attenuation is based on the B.C. kappa value of 0.011 s (Atkinson 1995*b*).

The available ground-motion database used to validate the seismological models for B.C. events was, until the introduction of the new GSC three-component broadband network a few years ago, comprised of vertical-component data; however, it is the horizontal component of motion that is of engineering interest. Fortunately, the horizontal and vertical components of ground motion are highly correlated; they can be related through a frequency-dependent ratio (*H*/*V* ratio) that is, for practical purposes, independent of magnitude and distance (e.g., Atkinson 1993). The *H*/*V* ratio depends primarily on site conditions, since near-surface changes in seismic impedance amplify horizontal motions significantly, while leaving vertical component motions largely unaffected (Theodulidis et al. 1996; Castro et al. 1997). The *H*/*V* ratio for hard-rock seismograph sites in B.C., which were used to derive

Fig. 6. Target 1/500 p.a. UHS from GSC for Vancouver (filled squares) and Victoria (open squares), and spectra of selected compatible time histories, multiplied by the stated scaling factor (the geometric average of the spectra for two horizontal components for the stated **M** and *R* combination is plotted). Solid line shows spectra for event that matches the short-period end of the spectrum; dotted line shows spectra for event that matches the long-period end of the spectrum.

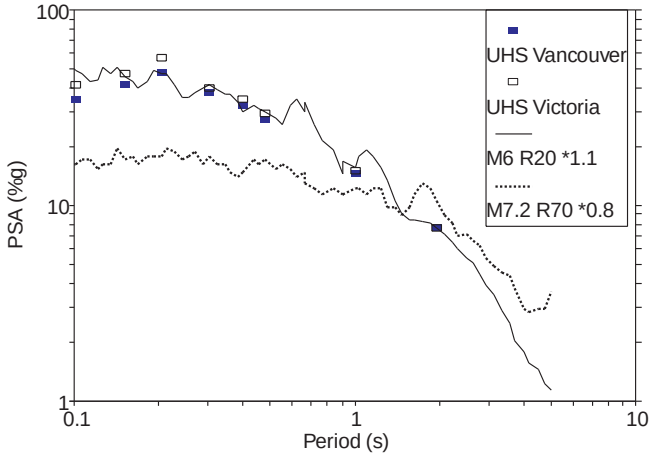

Fig. 7. Target 1/500 p.a. UHS from GSC for Tofino (filled squares), and spectra of selected compatible time histories, multiplied by the stated scaling factor (the geometric average of the spectra for two horizontal components for the stated **M** and *R* combination is plotted). Solid line shows spectra for event that matches the short-period end of the spectrum; dotted line shows spectra for event that matches the long-period end of the spectrum.

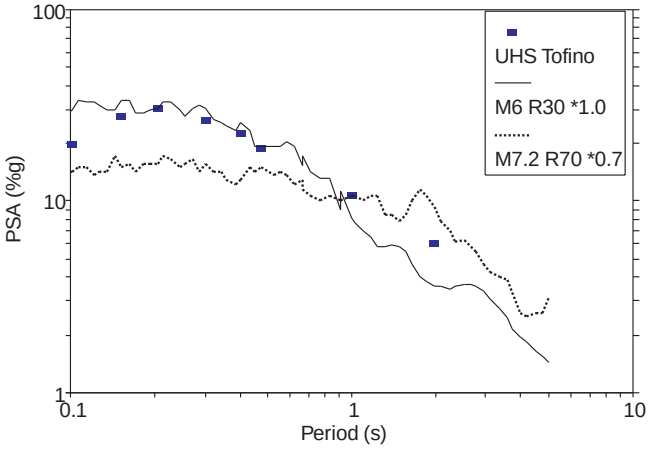

the regional ground-motion parameters needed for the simulations, was investigated using three-component broadband records of the Duvall earthquake and its aftershocks (Atkinson 1997); this investigation confirmed the applicability of the adopted model parameters for the horizontal component of shear radiation. Finally, the fundamental similarities and differences of the vertical and horizontal components may be noted. *P*-waves converted from *S*-waves at the near-surface boundaries may contribute to the vertical component in a shear-wave window, while the horizontal component is dominated by the *S*-radiation. The converted *P*-wave will nevertheless retain all spectral characteristics of the initial *S*-wave. The vertical component can thus be used to represent the characteristics of *S*-wave propagation without loss of generality, provided the *H*/*V* ratio for the recording sites can be estimated.

Using the same procedure as for eastern Canada, the soil amplification factors of Fig. 1 are applied to the Fourier amplitude spectrum for hard rock, as is the factor of 2 applied to simulate motions larger than the median for the stated **M** and *R*. The main difference between the eastern and western motions, for a given **M** and *R*, is that the eastern motions have enhanced high-frequency radiation levels. This difference has been well established empirically (see Atkinson and Boore 1997*b*).

The procedure used to determine the scenario events for each city, listed in terms of **M** and *R* in Table 1, is the same as that used for eastern Canada. Figures 6–8 show the target UHS for the B.C. cities and the average of the selected time histories, scaled by the stated fine-tuning factors. Again, there are two scenarios for each target spectrum, with two random horizontal components for each scenario, for a total of four time histories corresponding to each city. Time history analyses should be performed for all four scenario events for the target spectrum, in order to ensure compatibility. Figure 9 shows example B.C. time histories. The differences in frequency content between eastern and western motions, and its effects on peak ground acceleration, are apparent by comparing Figs. 5 and 9.

Simulations for cascadia subduction earthquake

Extension of point-source model to finite faults

The validity of the point-source model tends to break down near the source of large earthquakes, for which the effects of source–receiver geometry and rupture directivity can be significant. To model ground motions from a great earthquake on the Cascadia subduction zone, then, requires a simulation method that incorporates these finite-fault effects. In a finite-fault simulation, the large fault plane representing a great Cascadia earthquake is subdivided into smaller parts, each of which is treated as a point source, and the ground motions at a specified site are obtained by summing the delayed contributions from all parts of the fault (Hartzell 1978; Kanamori 1979; Heaton and Hartzell 1989). The shear-wave components of the seismic radiation are simulated using the procedures given by Beresnev and Atkinson (1997). Briefly, every subevent is associated with a stochastic point source, with parameters as described in the previous section. The initiation time of rupture at each subfault is determined by the propagation speed of the rupture, as it travels outward radially from the hypocentre. Heterogeneity of rupture is provided by adding a small random component to the starting time of rupture for each of the subfaults. Each subsource is allowed to trigger a number of times in order to provide the correct amount of final slip. This number is adjusted to conserve the total seismic moment of the simulated event. The radiation from each subfault is attenuated, using the point-source attenuation model, according to the distance between the subfault and the site. The total motions at the site contain the summed contributions from all subsources, appropriately lagged in time according to the geometry of rupture propagation.

The basic assumptions of this study can be compared with

Fig. 8. Target 1/500 p.a. UHS from GSC for Prince George (filled squares), and spectra of selected compatible time histories, multiplied by the stated scaling factor (the geometric average of the spectra for two horizontal components for the stated **M** and *R* combination is plotted). Solid line shows spectra for event that matches the short-period end of the spectrum; dotted line shows spectra for event that matches the long-period end of the spectrum.

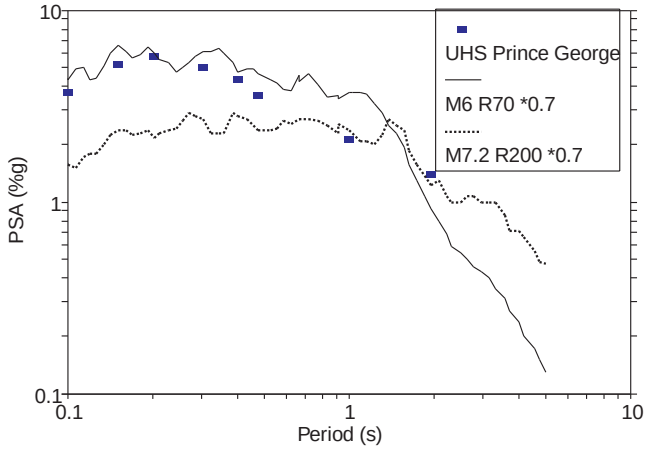

those of previous predictions of ground motion from a hypothetical megathrust earthquake on the Cascadia subduction zone. There are four such predictions available in the literature, all for the Seattle region (Youngs et al. 1988; Heaton and Hartzell 1989; Silva et al. 1990; Cohee et al. 1991). Youngs et al. (1988) used a theoretical source function to describe movement on the elementary subfaults. Heaton and Hartzell (1989) and Cohee et al. (1991) used recordings from smaller earthquakes as empirical source functions. The procedure of this study, and that of Silva et al., is based on a stochastic point-source representation of the subfault radiation. The approaches of Youngs et al., Heaton and Hartzell, and Cohee et al. all require specification of a detailed crustal structure, because they use theoretical attenuation based on wave propagation through the crustal structure. By contrast, the adopted modeling procedure, and that of Silva et al., employs an empirical attenuation operator. Overall, the simulation method employed in this study is closest to that of Silva et al. (1990), although the approach differs considerably in defining the basic physical parameters of the elementary sources. The advantage of the adopted simulation method is that it minimizes the use of poorly known model parameters (such as source–time functions or detailed crustal structure), by replacing them with well-tested empirical representations. For example, the source radiation is modeled with a general point-source spectrum rather than through records of small earthquakes; the latter rarely represent exact source conditions at the location of interest. Similarly, instead of relying on a crustal structure model which is not known in much detail, path effects are modeled through a region-specific empirical attenuation and duration model, which takes into account the general characteristics of wave propagation from hundreds of local earthquakes.

The adopted finite-fault simulation method has been successfully tested against observed near-field ground motions at rock sites from the **M**8.0 1985 Michoacan, Mexico, the **M**8.0 1985 Valparaíso, Chile, and the **M**5.8 1988 Saguenay, Quebec, earthquakes (Beresnev and Atkinson 1997). The level of

Fig. 9. Example time histories (unscaled) for western cities: (*a*) **M**6 event at $R = 20$ km and (*b*) **M**7.2 event at $R = 70$ km.

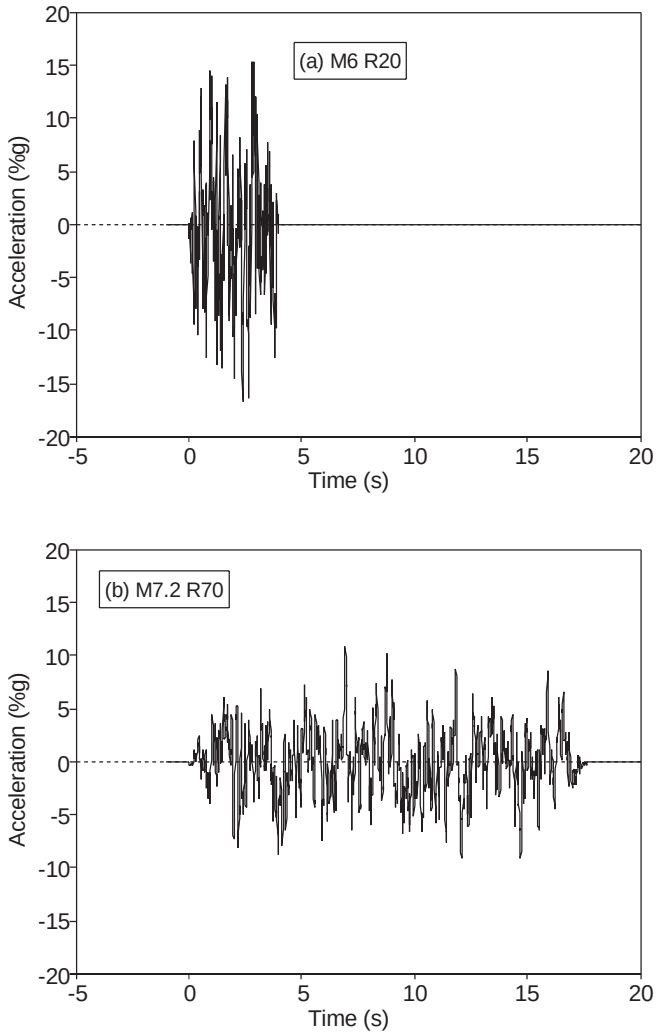

modeled low-frequency amplitudes is well constrained by the conservation of moment of the target event. The high-frequency level is principally controlled by the corner frequency of the subfault spectra, which is related to the subfault dimensions. Validation studies showed that the model defined in this way successfully reproduces recorded ground motions from **M** ~ 8.0 subduction-zone events at periods of 0.1–4 Hz (Beresnev and Atkinson 1997, Figs. 6 and 10), which covers most of the frequency range of engineering interest. An accuracy of 10% to 20% for specified ruptures is achieved, limited chiefly by the unpredictability of the geometry and rupture parameters of future earthquakes.

Subduction scenario

Hyndman and Wang (1995) used a compilation of geodetic, gravity, and thermal data to place constraints on the spatial extension of possible rupture for future Cascadia subduction zone earthquakes. The seismogenic zone was divided into two principal areas: (*i*) the fully locked zone, which is accumulating strain and will eventually rupture, due to exceedence of the material strength; and (*ii*) the transition zone, which allows

Fig. 10. The Cascadia subduction zone of western North America. The areas of the locked and transition zones on the subduction thrust fault are shown after Hyndman and Wang (1995). The surface projection of the fault plane for the scenario **M**8.5 earthquake is indicated by a rectangle.

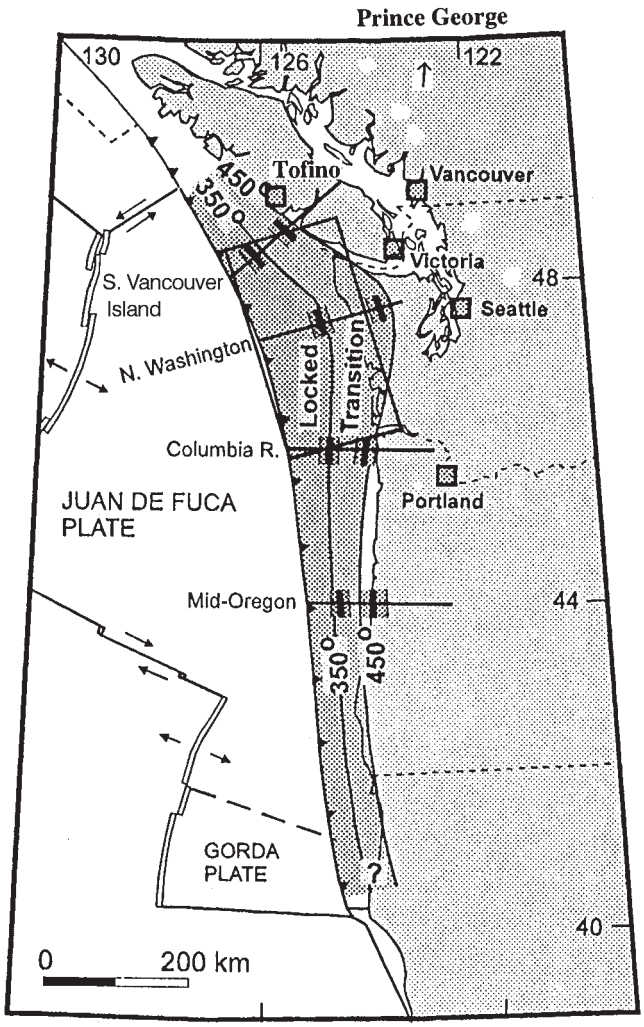

limited aseismic creep due to plasticity induced by rising temperatures. Below the transition zone, high temperatures cause free slip that prevents strain accumulation, limiting the downward extent of the seismogenic zone. Figure 10 shows the structure of the seismogenic zone as inferred by Hyndman and Wang (1995). Stippled areas bounded by solid lines show the locked and transition zones derived from geodetic data, and the thick short lines show their limits inferred from thermal analysis, with the bands indicating estimated uncertainties. Critical temperatures of 350°C and 450°C correspond to the onset of plasticity and the free-slip regimes, respectively. The widths of the locked and transition zones range from 35 + 35 km for central Oregon to northern California, to 90 + 90 km for the northern Washington profile. The southern Vancouver Island margin has widths of 60 + 60 km. The authors infer the short downdip extension of the Cascadia seismogenic zone, compared to other subduction zones, which they attribute to the peculiarities of the regional thermal regime.

The narrow width of the seismogenic zone limits the maximum earthquake size. However, Hyndman and Wang (1995) estimated that events of moment magnitude over 8 are possible. If the whole Cascadia seismogenic zone (including all of the locked and transition zones) fails in a single event, empirical fault-area versus magnitude relations would suggest an earthquake of about magnitude 9. In the simulations of this study, we adopt the magnitude **M** = 8.5.

Table 2. Modeling parameters for hypothetical Cascadia great earthquake.

Parameter	Value
Fault orientation	Strike 340°, dip 10°
Fault dimensions along strike and dip (km)	300 by 160
Depth range (km)	5–33
Magnitude	8.5
Moment (dyne-cm)[a]	6.3×10^{28}
Stress parameter (bar)[b]	30
Subfault dimensions (km)	25 by 20
Subfault moment (dyne-cm)	3.4×10^{26}
Number of subfaults on fault plane	96
Number of subsources summed	192
Subfault rise time (s)	3.2
Subfault corner frequency (Hz)	0.08
Distance-dependent duration, T_d (s)	1.4 ($R \leq 50$ km) $-2.1 + 0.07R$ ($R > 50$ km)
$Q(f)$	$380f^{0.39}$
Geometric spreading	$1/R$
Windowing function	Boxcar
f_m (Hz)	15
Crustal shear-wave velocity (km/s)	3.7
Crustal density (g/cm^3)	2.8

[a] 1 dyne = 10 μN.
[b] 1 bar =100 kPa.

The scenario **M**8.5 earthquake breaks the maximum width of the seismogenic zone, covering both the locked and the transition zones, thus representing the maximum hazard to the cities of western British Columbia. The fault area is 300 km along strike and 160 km downdip (Fig. 10), with strike and dip of 340° and 10°, respectively. The upper edge of the fault is at a depth of 5 km. Further extension of the fault plane to the north is not warranted by the geophysical data, while an extension to the south will not affect ground motions in the areas of interest.

To represent uncertainty in the pattern of strain release in future earthquakes, four possible rupture scenarios are considered. In the first model, the slip is distributed homogeneously over the fault plane. In the second and third models, 75% of the slip occurs in the upper and lower half of the fault, respectively. In these three cases, the rupture initiates at the centre of the fault. To model the effects of unilateral rupture propagation (which produces the strongest directivity effects), a fourth model is considered, in which rupture starts at the upper southern corner of the fault and propagates towards the north, with a slip distribution identical to that of model 3.

Ground motions for the scenario Cascadia ruptures are simulated for Vancouver, Victoria, Tofino, and Prince George. Their locations with respect to the fault are indicated in Fig. 10.

Fig. 11. Five-percent-damped pseudo-acceleration (PSA) response spectra and acceleration time histories for the **M**8.5 hypothesized Cascadia subduction zone earthquake for (*a*) Vancouver, (*b*) Victoria, (*c*) Tofino, and (*d*) Prince George. Response spectra and time histories are shown for the four rupture scenarios explained in the text. Peak ground accelerations in cm/s^2 are shown above each accelerogram. All curves are generated for the Class B "firm ground" condition. The thick solid lines on the response spectral plots show the ground motion estimates for a **M**8.2 Cascadia earthquake adopted by Adams et al. (1996).

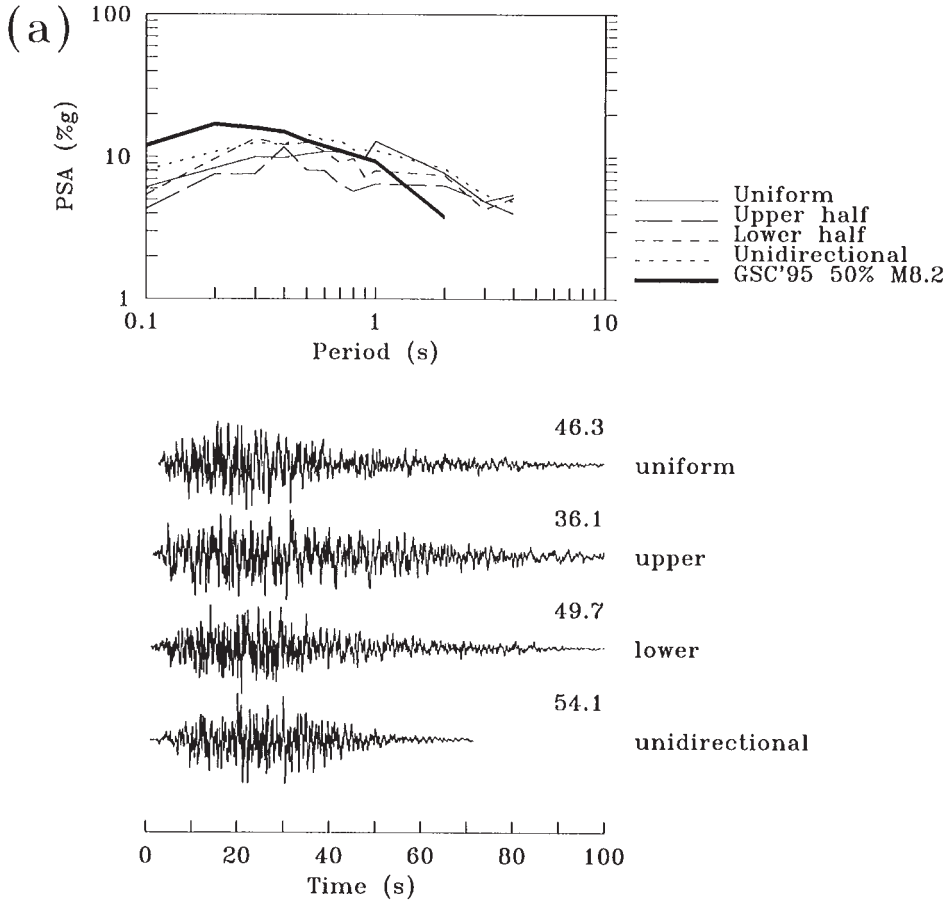

Parameters for simulations

The model parameters for the Cascadia subduction simulations are summarized in Table 2. The fault is discretized into 96 elements, 25 by 20 km each. Summation of 192 subsources is required to obtain the target moment; the number of triggerings of individual subfaults is controlled by an individual slip-distribution scenario (Beresnev and Atkinson 1997, p. 71). The stress parameter controlling the relationship between moment and slip on a subfault (static stress drop) is 30 bars (1 bar = 10^5 N/m^2), or the average value for subduction-zone events (Kanamori and Anderson 1975). This value agrees well with inferred Brune stress drops for regional earthquakes (Dewberry and Crosson 1995; Atkinson 1995*a*). Note that the stress-parameter value is not critical to the analysis; it is used only to assign moment to subevents (Beresnev and Atkinson 1997, pp. 71, 82). Empirical distance-dependent duration T_d, path attenuation Q, and geometric spreading models match those used in the western point-source simulations; they are well constrained by hundreds of earthquake recordings from the Cascadia region (Atkinson 1995*a*).

The adopted high-frequency spectral cut-off parameter f_m is 15 Hz, characteristic of western North America (Boore 1983). As for the crustal earthquake simulations above, amplification for Class B ground conditions is included, using the multiplicative factors of Fig. 1. Note that the ground response for the Cascadia scenario (and all other simulations) is assumed linear, since the peak acceleration levels generated in the simulations do not generally exceed the threshold for the onset of appreciable nonlinear behavior, which is between 100 and 200 cm/s^2 for soft soils and larger for firm soils (Beresnev and Wen 1997).

Response spectra and time histories

Figures 11*a*–11*d* present 5% damped pseudo-acceleration response spectra and acceleration time histories for the **M**8.5 Cascadia subduction zone earthquake for Vancouver, Victoria, Tofino, and Prince George, all for Class B sites. Response spectra at each site are shown for the four rupture scenarios described above, illustrating scatter of ground-motion characteristics due to uncertainty in the slip distribution and hypocentre for future events. Also given in Fig. 11 are the median (50th percentile) response spectra estimated by Adams et al. (1996) for a **M**8.2 Cascadia subduction earthquake, which were based on the empirical ground-motion relationships of Crouse (1991). Note that the Adams et al. spectra are not target spectra in this case. The object of the simulations is to model the

Fig. 11 (*continued*).

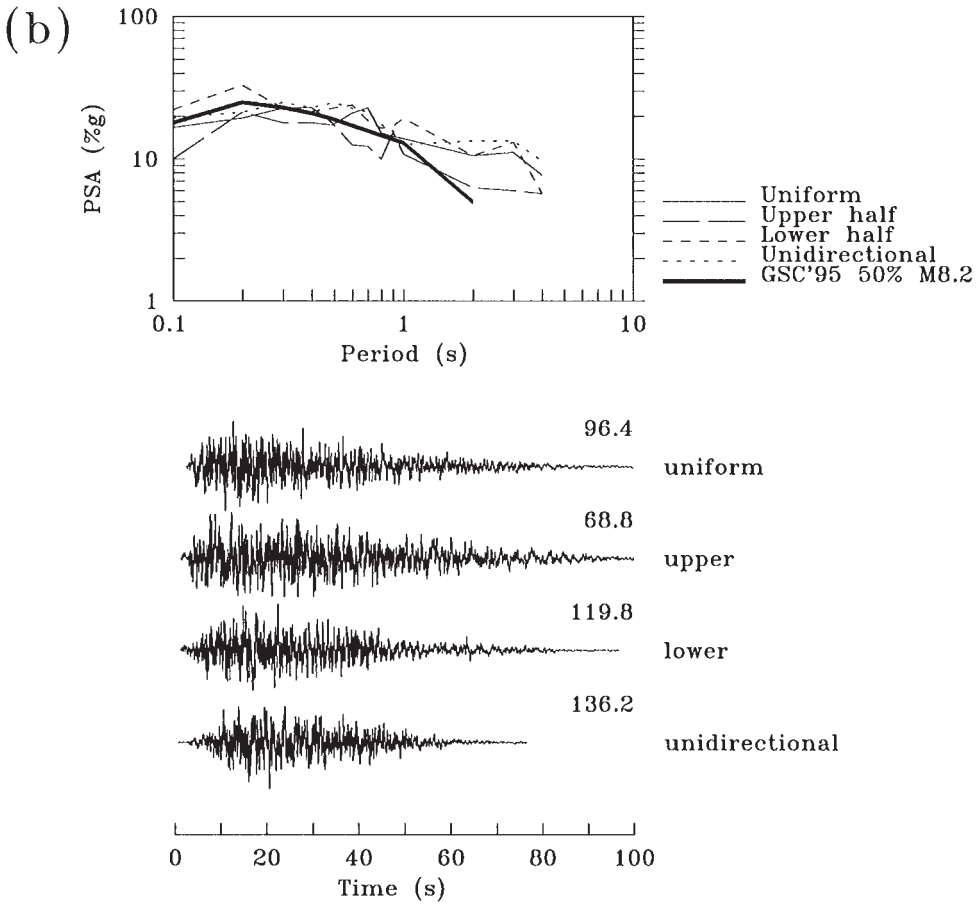

motions from a Cascadia subduction earthquake in a more physical and region-specific manner than can be achieved by simply applying a global attenuation relationship. The spectra of Adams et al. are thus provided for comparison, rather than as a target.

Figures 11*a*–11*d* suggest that the uncertainty in the response spectral values caused by a variety of possible earthquake scenarios does not exceed a factor of 2 on average. The highest spectral amplitudes for the Cascadia earthquake are predicted for Tofino, located just north of the projection of the fault plane. Ground-motion durations at Vancouver and Victoria are of the order of 80–90 s, for a hypocentre located near the centre of the fault; durations are only about 40 s at Tofino, due to its position along the strike of the fault plane. Durations are conspicuously shorter and spectral amplitudes generally higher in all locations for the case of unilateral north–south rupture; this is a pure directivity effect. Slip concentration in the lower half of the fault also leads to generally higher amplitudes of motion, because of the proximity of the lower part of the subduction zone to the coastal areas and its low dip angle.

The spectra of the simulated ground motions are fairly consistent with those given by the global empirical relations used by GSC, for Vancouver, Victoria, and Tofino. The GSC spectra are slightly lower at long periods, which may be partly attributable to the lower moment of the target event used by the GSC. It should be noted that the GSC spectra are not well constrained at long periods, since reliable empirical data are lacking at long periods in the underlying Crouse (1991) database. This study therefore suggests that the GSC spectra for the Cascadia subduction scenario may be unconservative at long periods. The spectra are essentially identical in the intermediate-period range. The agreement is best for Victoria and Tofino, the locations closest to the fault. The remaining discrepancies may reflect differences in regional attenuation between Cascadia and other subduction regimes, since the empirical relations used by GSC (Crouse 1991) are based on ground-motion data from other subduction zones around the world.

There is almost an order of magnitude difference between our predictions for Prince George and those of the GSC at short periods, whereas the curves converge at long periods. Our result is readily understood in terms of frequency-dependent anelastic attenuation (Q-factor), which prevents high frequencies from propagating to very long distances (Prince George is hundreds of kilometres from the fault rupture). The shape of the response spectra necessarily changes with distance, with the maxima shifting to longer periods as the signal propagates. This feature can be seen from a comparison of Fig. 11*d* with Figs. 11*a*–11*c*, and is noted in empirical studies throughout the world (e.g., Boore et al. 1993; Atkinson and Boore 1995, 1997*a*). It is puzzling that this behavior is not seen in the GSC spectra, where the response spectral shape remains essentially unchanged by the effects of attenuation; this suggests that there

Fig. 11 (*continued*).

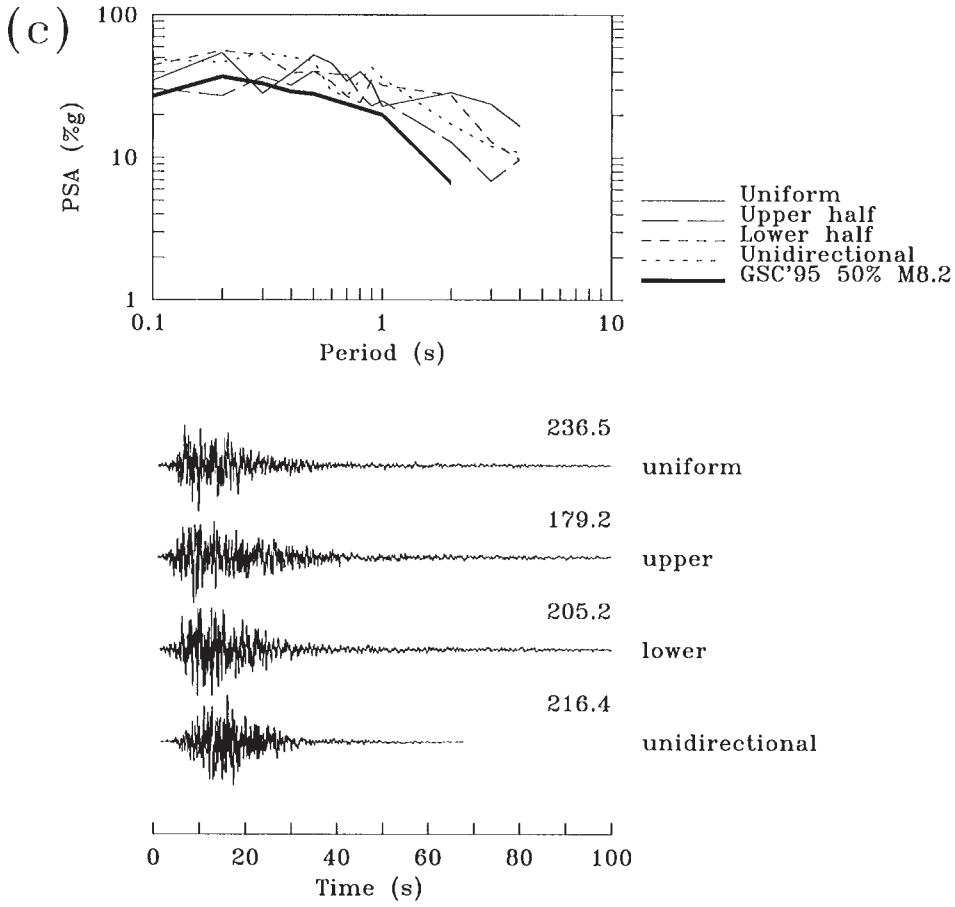

may be a basic problem with applying the empirical Crouse relations to large distances. The synthetic accelerograms for Prince George have a distinct low-frequency content (Fig. 11*d*); the duration for the first three scenarios is greater than 100 s, due to the long crustal path. Peak ground accelerations do not exceed 4.5 cm/s^2, and the difference in response spectra for the four scenarios is negligible.

Conclusions

Ground-motion time histories, which are compatible with the 1/500 p.a. uniform hazard spectra provided by the new national seismic hazard maps of the Geological Survey of Canada (Adams et al. 1996), have been simulated for selected Canadian cities. The simulations provide a realistic representation of ground motion for the earthquake magnitudes and distances that contribute most strongly to hazard at the selected cities. Engineering analyses by time-history methods can be performed for structures in these cities simply by using the simulated records indicated in Table 1 (4 records are required for each location), scaled by multiplying every point by the "fine-tuning" factors given in Table 1. These records, based on point-source simulations of crustal (and in some cases subcrustal) earthquake sources, have spectra that match the target 1/500 p.a. UHS of the new national seismic hazard maps, when considered as a suite. The simulated records have amplitudes and frequency content that are consistent with seismological observations for earthquakes within the specific regions.

For western cities, there is an additional hazard due to the possible occurrence of great earthquakes on the Cascadia subduction zone. Simulated time histories are provided at selected western cities for a scenario event of **M**8.5 on the subduction zone, using a finite-fault simulation methodology to consider the variability in motions due to different possible rupture scenarios.

The ground motions simulated for the scenario **M**8.5 subduction event are not associated with a specific probability level. Current information (Atwater et al. 1995) suggests that the probability of these ground motions is comparable to that of the 1/500 p.a. UHS generated for the new national seismic hazard maps (the maps do not specifically include the Cascadia subduction hazard). Thus it would be within the spirit of the hazard maps to perform engineering analyses for buildings in western cities for both the crustal time histories given in Table 1 and the Cascadia scenario time histories. All time histories generated in this study are available free of charge to interested parties, by sending an addressed, formatted 3.5" disk to the first author, or by e-mail to gma@ccs.carleton.ca.

On a cautionary note, the time histories reflect a seismological evaluation conducted at a regional overview level, consistent with the NBCC spectra. They are not intended to replace detailed site-specific seismological studies for important structures, for which seismic design may be a major engineering

Fig. 11 (*concluded*).

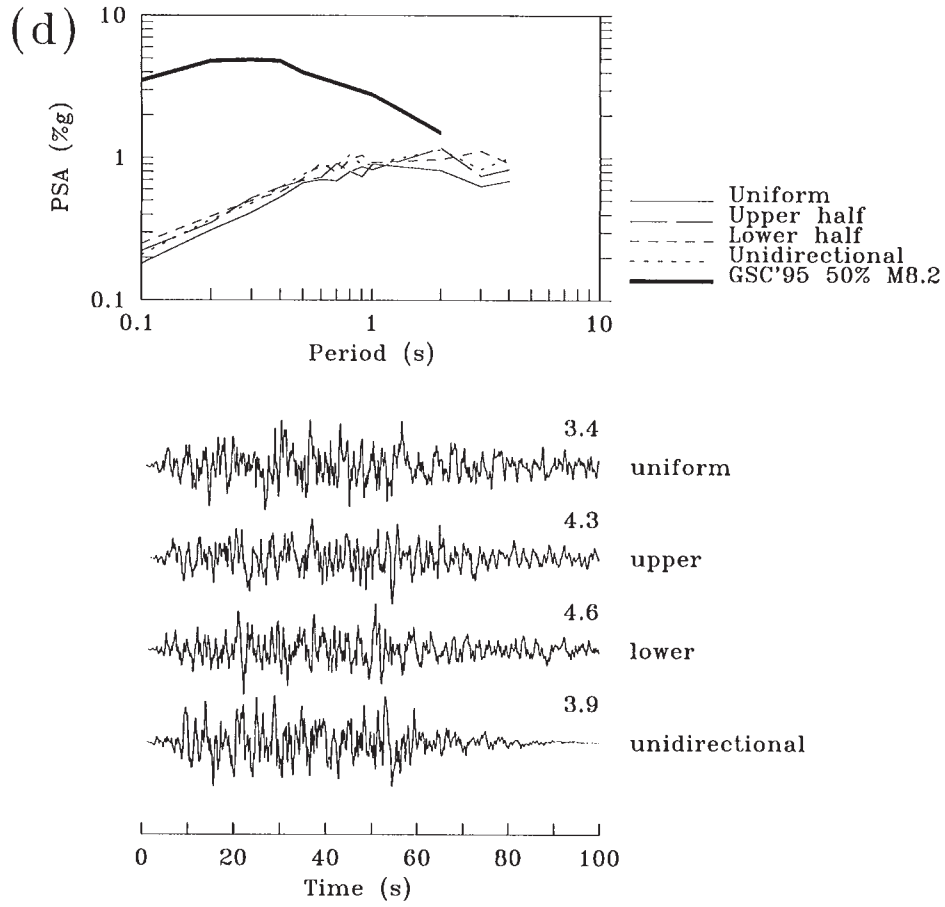

and economic factor. In such cases, time histories can more appropriately be developed as a component of a comprehensive site-specific seismic hazard analysis.

Acknowledgements

This research was funded by the Natural Sciences and Engineering Research Council of Canada. Two anonymous reviewers for the journal provided constructive comments.

References

Adams, J., Weichert, D., Halchuk, S., and Basham, P. 1996. Trial seismic hazard maps of Canada — 1995: final values for selected Canadian cities. Geological Survey of Canada, Ottawa, Ont., Open File 3283.

Atkinson, G. 1990. Updated seismic hazard estimates at Ontario Hydro sites. Report, Ontario Hydro, Toronto, Ont.

Atkinson, G. 1991. Use of the uniform hazard spectrum in characterizing expected levels of seismic ground shaking. Proceedings of the 6th Canadian Conference on Earthquake Engineering, Toronto, Ont., pp. 469–476.

Atkinson, G. 1993. Notes on ground motion parameters for eastern North America: duration and *H*/*V* ratio. Bulletin of the Seismological Society of America, **83**: 587–596.

Atkinson, G. 1995*a*. Attenuation and source parameters of earthquakes in the Cascadia region. Bulletin of the Seismological Society of America, **85**: 1327–1342.

Atkinson, G. 1995*b*. The high-frequency shape of the source spectrum for earthquakes in eastern and western Canada. Bulletin of the Seismological Society of America, **85**: 106–112.

Atkinson, G. 1997. Empirical ground motion realtions for earthquakes in the Cascadia region. Canadian Journal of Civil Engineering, **24**: 64–77.

Atkinson, G., and Boore, D. 1995. New ground motion relations for eastern North America. Bulletin of the Seismological Society of America, **85**: 17–30.

Atkinson, G., and Boore, D. 1997*a*. Stochastic point-source modeling of ground motions in the Cascadia region. Seismological Research Letters, **68**: 74–85.

Atkinson, G., and Boore, D. 1997*b*. Some comparisons between recent ground motion relations. Seismological Research Letters, **68**: 24–40.

Atwater, B., Nelson, A., Clague, J., Carver, G., Yamaguchi, D., Bobrowsky, P., Bourgeois, J., Darienzo, P., Grant, W., Hemphill-Haley, E., Kelsey, H., Jocoby, G., Nishenko, S., Palmer, S., Peterson, C., and Reinhart, M. 1995. Summary of coastal geologic evidence for past great earthquakes at the Cascadia subduction zone. Earthquake Spectra, **11**: 1–18.

Beresnev, I., and Atkinson, G. 1997. Modeling finite fault radiation from the ω^n spectrum. Bulletin of the Seismological Society of America, **87**: 67–84.

Beresnev, I., and Wen, K. 1997. Nonlinear ground response — a reality? Bulletin of the Seismological Society of America, **86**: 1964–1978.

Boore, D. 1983. Stochastic simulation of high-frequency ground motions based on seismological models of the radiated spectra. Bulletin of the Seismological Society of America, **73**: 1865–1894.

Boore, D., Joyner, W., and Fumal, T. 1993. Estimation of response

spectra and peak accelerations from western North American earthquakes: an interim report. U.S. Geological Survey Open-file Report 93-509.

Castro, R., Mucciarelli, M., Pacor, F., and Petrungaro, C. 1997. S-wave site-response estimates using horizontal-to-vertical spectral ratios. Bulletin of the Seismological Society of America, **87**: 256–260.

Cohee, B., Somerville, P., and Abrahamson, N. 1991. Simulated ground motions for hypothesized Mw = 8 subduction earthquakes in Washington and Oregon. Bulletin of the Seismological Society of America, **81**: 28–56.

Cornell, C. 1968. Engineering seismic risk analysis. Bulletin of the Seismological Society of America, **58**: 1583–1606.

Crouse, C. 1991. Ground-motion attenuation equations for Cascadia subduction zone earthquakes. Earthquake Spectra, **7**: 201–236.

Dewberry, S., and Crosson, R. 1995. Source scaling and moment estimation for the Pacific Northwest Seismograph Network using S-coda amplitudes. Bulletin of the Seismological Society of America, **85**: 1309–1326.

EERI Committee on Seismic Risk. 1989. The basics of seismic risk analysis. Earthquake Spectra, **5**: 675–702.

EPRI. 1986. Seismic hazard methodology for the central and eastern United States. Electric Power Research Institute, Palo Alto, Calif., Report NP-4726.

Greig, G., and Atkinson, G. 1993. The damage potential of eastern North American earthquakes. Seismological Research Letters, **64**: 119–137.

Hanks, T., and McGuire, R. 1981. The character of high-frequency strong ground motion. Bulletin of the Seismological Society of America, **71**: 2071–2095.

Hartzell, S. 1978. Earthquake aftershocks as Green's functions. Geophysics Research Letters, **5**: 1–14.

Heaton, T., and Hartzell, S. 1989. Estimation of strong ground motions for hypothetical earthquakes on the Cascadia subduction zone, Pacific Northwest. Pure Applied Geophysics, **129**: 131–201.

Heidebrecht, A.C., Naumoski, N., and Rutenberg, A. 1994. Towards a new base shear format in future NBCC seismic provisions. Canadian Journal of Civil Engineering, **21**: 682–695.

Hyndman, R., and Wang, K. 1995. The rupture zone of Cascadia great earthquake from current deformation and the thermal regime. Journal of Geophysical Research, **100**(B11): 22 133 – 22 154.

Kanamori, H. 1979. A semi-empirical approach to prediction of long-period motions from great earthquakes, Bulletin of the Seismological Society of America, **69**: 1645–1670.

Kanamori, H., and Anderson, D. 1975. Theoretical basis of some empirical relations in seismology. Bulletin of the Seismological Society of America, **65**: 1073–1095.

Martin, G., and Dobry, R. 1994. Earthquake site response and seismic code provisions. National Center for Earthquake Engineering, Buffalo, N.Y., Quarterly Bulletin, **8**(4): 1–6.

McGuire, R. 1977. Seismic design spectra and mapping procedures using hazard analysis based directly on oscillator response. International Journal of Earthquake Engineering and Structural Dynamics, **5**: 211–234.

McGuire, R. 1995. Probabilistic seismic hazard analysis and design earthquakes: closing the loop. Bulletin of the Seismological Society of America, **85**: 1275–1284.

NEHRP. 1994. NEHRP recommended provisions for seismic regulations for new buildings. Part 1: provisions. Building Seismic Safety Council, Washington, D.C.

Reiter, L. 1990. Earthquake hazard analysis. John Wiley & Sons, Inc., New York.

Silva, W., Darragh, R., and Wong, I. 1990. Engineering characterization of earthquake strong ground motions with applications to the Pacific Northwest. *In* Proceedings of the Third NEHRP Workshop on Earthquake Hazards in the Puget Sound/Portland Region. *Edited by* W. Hays. U.S. Geological Survey Open-file Report.

Theodulidis, N., Bard, P., Archuleta, R., and Bouchon, M. 1996. Horizontal-to vertical spectral ratio and geological conditions: the case of Garner Valley downhose array in southern California. Bulletin of the Seismological Society of America, **86**: 306–319.

Toro, G., and McGuire, R. 1987. Calculational procedures for seismic hazard analysis and its uncertainty in the eastern United States. Proceedings of the Third International Conference on Soil Dynamics and Earthquake Engineering, Princeton, N.J., pp. 195–206.

Turkstra, C., and Tallin, A. 1988. A re-evaluation of design spectra for seismic damage control. National Center for Earthquake Engineering Research, State University of New York, Buffalo, N.Y., Report NCEER-88-0032.

Youngs, R., Day, S., and Stevens, J. 1988. Near field ground motions on rock for large subduction earthquakes. Proceedings of the 2nd Conference on Earthquake Engineering and Soil Dynamics, Geotechnical Division, American Society of Civil Engineers, Park City, Utah, June 27–30, pp. 445–462.